Articles

Metal Requirements and Phosphodiesterase Activity of tRNase Z Enzymes†

Bettina Späth,[⊥] Florian Settele,[⊥] Oliver Schilling,[‡,||] Igor D'Angelo,[#] Andreas Vogel,[‡,⊥,⊗] Ingo Feldmann,[§] Wolfram Meyer-Klaucke,[‡] and Anita Marchfelder*[,⊥]

Molekulare Botanik, Universität Ulm, Albert-Einstein-Allee 11, 89069 Ulm, Germany, EMBL Outstation Hamburg, Notkestrasse 85, 22603 Hamburg, Germany, ISAS - Institute for Analytical Sciences, Bunsen-Kirchhoff-Strasse 11, 44139 Dortmund, Germany, and Centre for Blood Research, Biochemistry Department, University of British Columbia, 2350 Health Sciences Mall, Vancouver, BC V6T 1Z3, Canada

Received May 29, 2007; Revised Manuscript Received October 4, 2007

ABSTRACT: The endonuclease tRNase Z from *A. thaliana* (AthTRZ1) was originally isolated for its tRNA 3′ processing activity. Here we show that AthTRZ1 also hydrolyzes the phosphodiester bond in bis(*p*-nitrophenyl) phosphate (bpNPP) with a k_{cat} of 7.4 s^{-1} and a K_M of 8.5 mM. We analyzed 22 variants of AthTRZ1 with respect to their ability to hydrolyze bpNPP. This mutational mapping identified fourteen variants that lost the ability to hydrolyze bpNPP and seven variants with reduced activity. Surprisingly, a single amino acid change (R252G) resulted in a ten times higher activity compared to the wild type enzyme. tRNase Z enzymes exist in long and short forms. We show here that in contrast to the short tRNase Z enzyme AthTRZ1, the long tRNase Z enzymes do not have bpNPP hydrolysis activity pointing to fundamental differences in substrate cleavage between the two enzyme forms. Furthermore, we determined the metal content of AthTRZ1 and analyzed the metal requirement for bpNPP hydrolysis. AthTRZ1 shows a high affinity for Zn^{2+} ions; even upon incubation with metal chelators, 0.76 Zn^{2+} ions are retained per dimer. In contrast to bpNPP hydrolysis, pre-tRNA processing requires additional metal ions, Mn^{2+} or Mg^{2+}, as Zn^{2+} ions alone are insufficient.

The tRNA endonuclease tRNase Z has been shown to catalyze tRNA 3′ end processing *in vitro* and *in vivo* (for a review see ref *1*). The first tRNase Z, AthTRZ1,[1] was isolated from *Arabidopsis thaliana* (*2*). Subsequent database analyses showed that AthTRZ1 homologues are present in organisms of all three domains: bacteria, archaea, and eukarya. The tRNase Z family of proteins can be divided into two subgroups: the short tRNase Z proteins (250−350 amino acids long) termed tRNase Z^S, and the long tRNase Z proteins (700 to 950 amino acids), the tRNase Z^L enzymes. Whereas the tRNase Z^S proteins are present in all kingdoms, tRNase Z^L enzymes are only found in eukarya. Both subgroups are part of the same protein family since the C-terminal part of the tRNase Z^L proteins has high sequence similarity to the tRNase Z^S enzymes. The short tRNase Z enzymes are active as homodimers, supporting the proposal that duplication of the gene for the short protein resulted in the long tRNase Z gene (*3*).

From respective sequence similarities the tRNase Z enzymes were classified as belonging to the family of metal-dependent β-lactamases (*3*), a group of metalloproteins which perform a variety of diverse functions (*4*−*6*). Metal-dependent β-lactamases have highly diverse sequences but all share a common structural motif, the β-lactamase fold. The β-lactamase fold consists of external α-helices that enclose two layers of β-sheets. The recently published crystal structure of the tRNase Z enzymes from *Bacillus subtilis* (*7*), *Thermotoga maritima* (*8*), and *Escherichia coli* (*9*) confirm that the tRNase Z enzymes belong to the family of metal-dependent β-lactamases since they indeed contain the metallo-β-lactamase fold.

The metal-dependent β-lactamase family has been classified into 16 subgroups (*6*). The tRNase Z enzymes belong to the Elac1/Elac2 subgroup. Other subgroups include the 3′ mRNA cleavage and adenylation specificity factors (CPSF) (*10*), SNM1 (also named PSO2), and Artemis (*11*, *12*), proteins involved in DNA repair. Another subgroup consists of cAMP phosphodiesterase enzymes (*13*) that catalyze the hydrolysis of cAMP to the corresponding nucleoside 5′ monophosphate.

† This work was supported by the VolkswagenStiftung and the DFG.

* Corresponding author: Tel : +49 731 5022658, Fax: +49 731 5022626, E-mail: anita.marchfelder@uni-ulm.de.

[⊥] Universität Ulm.

[‡] EMBL Outstation Hamburg.

[§] Institute for Analytical Sciences.

[#] University of British Columbia.

[||] Present address: The UBC Centre for Blood Research, Departments of Oral Biological & Medical Sciences, and Biochemistry and Molecular Biology, University of British Columbia, Vancouver, B.C., Canada, V6T 1Z3.

[⊗] Present address: c-LEcta GmbH, Deutscher Platz 5b, 04103 Leipzig, Germany.

[1] Abbreviations: AthTRZ1, *Arabidopsis thaliana* tRNase Z^{S1}; bpNPP, bis(*p*-nitrophenyl) phosphate; EMSA, electrophoretic mobility shift assay.

10.1021/bi7010459 CCC: $37.00
Published on Web 12/04/2007

Generally metallo-β-lactamases bind one or two metal ions, preferably zinc, iron, or manganese (*4*). Metal ions as part of metalloproteins are essential for numerous biocatalytic processes. In many cases metalloenzymes require very specific metal ions to achieve catalytic functionality, leading to the presumption that metalloproteins bind metal ions with high selectivity (*14*). Exceptions to this rule exist where promiscuous metal binding has been observed, for example glyoxalase II, a thiolesterase sharing the metallo-β-lactamase fold that is catalytically active with various ratios of iron, manganese, and zinc bound *in vivo* (*15*).

Hydrolytic proteins belonging to the metallo-β-lactamase family share the short sequence motif HxHxDH. The first two histidines and the aspartate are generally conserved metal binding ligands. The only tRNase Z enzyme for which the dependence of the catalytic activity on different metal ions has been detailed is the *E. coli* tRNase Z (EcoTrz); Meyer-Klaucke and his colleagues showed that the active form of EcoTrz has a binuclear metal binding site that holds zinc ions in the active form (*16*).

AthTRZ1 also contains the HxHxDH motif and as shown earlier *in vitro* tRNA processing reactions catalyzed by AthTRZ1 require Mn^{2+}, Ca^{2+}, or Mg^{2+}, whereas Zn^{2+} and Fe^{2+} do not activate the EDTA-treated enzyme (*17*, *18*). We have analyzed the identity and stochiometry of metal ions bound by AthTRZ1. Furthermore, we investigated the reactivity of wild type AthTRZ1 and 22 AthTRZ1 variants toward the small phosphodiester bpNPP. In addition we compared the tRNase Z activity toward the two substrates pre-tRNA and bpNPP to see whether the requirements for both substrates are the same.

EXPERIMENTAL PROCEDURES

Cloning and Expression of AthTRZ1 and Variants. AthTRZ1 and variants were cloned and expressed as described (*17*). Protein concentrations were determined by measuring A_{280} values and using calculated molar absorption coefficients (*19*).

Cloning of the tRNase Z Gene from Saccharomyces cerevisiae and Drosophila melanogaster. Cloning of the cDNAs and expression of the tRNase Z proteins from *S. cerevisiae* and *D. melanogaster* were performed as described (*20*, *21*).

Electrophoretic Mobility Shift Assay (EMSA) and Cross-Linking Experiments. Cross-linking experiments were carried out as described (*17*). For EMSA analyses, 1 fmol of ^{32}P-labeled wheat tRNA was incubated with 250 ng of recombinant protein in EMSA buffer (10 mM Tris-HCl pH 8.0, 10 mM KCl, 5 mM $MgCl_2$, 10 μg/mL BSA, 5% glycerol) for 20 min at room temperature. Samples were loaded on 8% nondenaturing polyacrylamide gels and run at constant voltage of 10 V cm^{-1} in 1x TGE (10 mM Tris pH 8, 58 mM glycine) at 4 °C. Gels were analyzed by autoradiography. For competition experiments bpNPP was added to the reaction to final concentrations of 1−15 mM bpNPP.

In Vitro tRNA Processing Assays. All processing assays were carried out with 100 ng of recombinant protein in a reaction volume of 100 μL in nuz-IVP buffer (40 mM Tris, pH 8.4, 2 mM $MgCl_2$, 2 mM KCl, and 2 mM dithiothreitol) at 37 °C for 30 min with 50 fmol of tRNA substrate if not stated otherwise. Substrates were labeled with α-^{32}P-UTP.

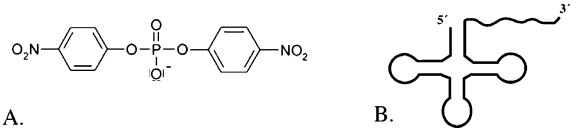

FIGURE 1: tRNase Z substrates. A. The chromogenic phosphodiester bis(*p*-nitrophenyl) phosphate (bpNPP), which is the smallest tRNase Z substrate known so far. B. Schematic drawing of a pre-tRNA substrate, containing the tRNA and a 3′ trailer.

Processing reactions were terminated by phenol and chloroform extractions. Nucleic acids were precipitated, and reaction products were analyzed on 8% polyacrylamide gels. Gels were analyzed by autoradiography.

For inhibition of the processing reaction bpNPP was added to the reaction to final concentrations of 1−17.5 mM.

Metal Dependence of the in Vitro Processing Reaction. To analyze which metal ions are required for the processing reaction, reactions were preincubated with 10 mM EDTA and 2 mM TPEN (tetrakris-(2-pyridylmethyl)ethylendiamine) at 4 °C for 3 h or overnight. Chelators and chelator−metal complexes were subsequently removed by dialysis. *In vitro* processing reactions were carried out in metal−IVP buffer (40 mM Tris, pH 8.5, 2 mM dithiothreitol), and different metal ions (0.2 mM Mn^{2+}; 2 mM Mg^{2+}) were added to analyze their effect on processing. No difference was observed whether the protein was preincubated with metal ions for 3 h at 24 °C or whether the reaction was started (by the addition of the tRNA precursor) immediately after the addition of the metal ions. All buffers were treated with Chelex 100 (Bio-Rad) to remove metal ions.

bpNPP Hydrolysis Assay and Kinetic Analysis. Phosphodiesterase activity was determined using the substrate bis(*p*-nitrophenyl) phosphate (bpNPP). Standard reaction conditions were 20 mM Tris/HCl, pH 7.4, and rising amounts of bpNPP (0−16 mM). Release of *p*-nitrophenol was continuously monitored for 3 min at 405 nm. The reaction rate was determined from initial slopes and the concentration of *p*-nitrophenol was calculated using the molecular extinction coefficient $\epsilon = 11\,500$ M^{-1} cm^{-1} (pH 7.4). One unit of activity corresponds to 1 μmol of *p*-nitrophenol liberated per min at 37 °C. The kinetic parameters were determined using Michaelis−Menten and the program Origin 7.0 (Microcal, Northhampton, MA). All reactions were carried out three times, and results were averaged. For inhibition with tRNA molecules, the bpNPP reaction was done with 20 μM bpNPP and 20 μM tRNA.

Metal Analysis. Proteins were depleted of metal by incubation with 10 mM EDTA and 2 mM TPEN at 4 °C for 3 h or over night. Chelators and chelator−metal complexes were subsequently removed by dialysis. All buffers were made with metal-free chemicals (confirmed by ICP-OES), and only new plasticware was used. For the subsequent reactions, different metal ions (0.2 mM Mn^{2+}, 0.02 mM Fe^{2+} or Zn^{2+}, 2 mM Mg^{2+}) were added as described in Results. To determine the final metal content, protein samples and dialysis buffers were analyzed by ICP−MS (ISAS - Institute for Analytical Sciences, Dortmund, Germany) and ICP-OES (GSF Neuherberg, Germany).

Molecular Docking. BpNPP was initially docked to *A. thaliana* tRNase Z by surface patch matching algorithms as implemented in the program Patchdock (*22*). Ten solutions were obtained and scored accordingly. The best solution was

Table 1: Kinetic Parameters of bpNPP Catalysis for EcoTrz, AthTRZ1, and Variants

protein	K_M (mM)	k_{cat} (s^{-1})	k_{cat}/K_M (s^{-1}/mM)
EcoTrz	4	59	15
AthTRZ1 wild type	8.5 ± 1.3	7.4 ± 0.5	0.9 ± 0.1
AthTRZ1-C25G	13.2 ± 2.1	3.9 ± 0.4	0.3 ± 0.02
AthTRZ1-C40G	6 *	3.1*	0.5*
AthTRZ1-F51L	6.5*	2.3*	0.4*
AthTRZ1-G62V	8*	0.8*	0.1*
AthTRZ1-P64A	22.2 ± 2.2	4.6 ± 0.3	0.2 ± 0.01
AthTRZ1-P178A	1.2 ± 0.2	1.8 ± 0.1	1.5 ± 0.2
AthTRZ1-E208A	3.5 ± 0.5	4.0 ± 0.2	1.2 ± 0.1
AthTRZ1-R252G	1.8 ± 0.3	68.5 ± 3.4	38.2 ± 5.1

[a] For AthTRZ1 and all variants, the kinetic parameters k_{cat}, K_M, and k_{cat}/K_M were determined. The data for EcoTrz are from Vogel et al. ±*16*). Data with a * are derived from measurements where no plateau was reached, and thus the highest kinetic value measured was taken. Consequently the error was not calculable and was estimated to be 20%.

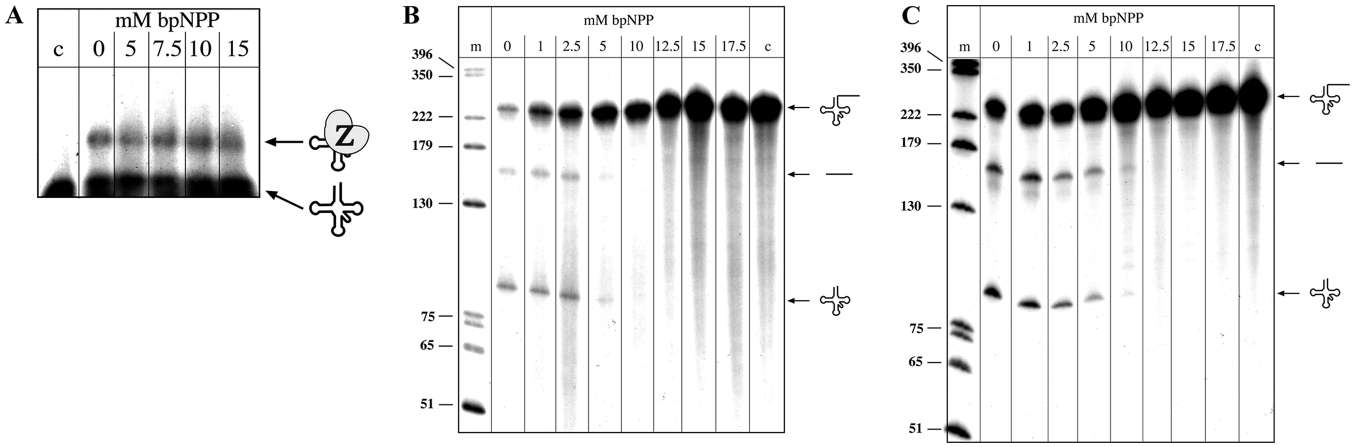

FIGURE 2: A. bpNPP does not inhibit tRNA binding. AthTRZ1 was incubated with wheat tRNA with and without bpNPP addition. The reaction was loaded onto a nondenaturing polyacrylamide gel, which was subsequently analyzed by autoradiography. The autoradiograph clearly shows that addition of bpNPP does not interfere with tRNA binding. Lane 0: AthTRZ1 incubated with tRNA, lanes 5, 7.5, 10 and 15: incubation of AthTRZ1 with tRNA and varying concentrations of bpNPP (concentrations given in mM above the lane); lane c: control without addition of proteins. The tRNA and the tRNA/protein complex are shown at the right schematically. B. bpNPP does inhibit pre-tRNA processing. Processing reactions were incubated with varying concentrations of bpNPP (lanes 1, 2.5, 5, 10, 12.5, 15, 17.5) and without (lane 0) (bpNPP concentrations given in mM above the lane). While tRNase Z normally processes the precursor tRNA (lane 0), incubation with bpNPP concentrations higher than 5 mM clearly inhibits the processing reaction. The loss of radioactivity in lanes 0−10 is a technical problem of incomplete redissolution of the RNA after precipitation of the tRNA processing reaction. Lane m: DNA size marker (sizes are indicated in nucleotides at the left); lane c: control reaction without addition of proteins. Precursor and products are shown schematically at the right. C. Long tRNase Z is inhibited by bpNPP. Processing reactions were incubated with varying concentrations of bpNPP (lanes 1, 2.5, 5, 10, 12.5, 15, 17.5) and without (lane 0) (bpNPP concentrations given in mM above the lane). While tRNase Z normally processes the precursor tRNA (lane 0), incubation with bpNPP concentrations higher than 10 mM clearly inhibits the processing reaction. Lane m: DNA size marker (sizes are indicated in nucleotides at the left); lane c: control reaction without addition of proteins. Precursor and products are shown schematically at the right.

identified as the most probable, placing the bpNPP molecule in close proximity to the Zn^{2+} ions of the active site. The initial bpNPP molecule was then manually translated/rotated to obtain optimal bond lengths and redocked to tRNase Z with multiple steps of energy minimization as implemented in the program DOCK 6 (*23*). All modeling, structure superposition, analysis, and visualization was performed with the program COOT (*24*).

RESULTS AND DISCUSSION

Different Substrates for Different tRNase Z Enzymes. Bis-(*p*-nitrophenyl) phosphate (bpNPP) is a chromogenic phosphodiester (Figure 1) and the smallest substrate known for the tRNase Z proteins so far. The first tRNase Z enzyme which was found to possess bpNPP cleavage activity was the *E. coli* tRNase Z (*16*). Since small phosphodiesters might be also *in vivo* substrates for the tRNase Z enzymes, we analyzed whether this phosphodiester molecule is a substrate for all tRNase Z enzymes. Therefore, we incubated it with the short tRNase Z enzyme from *A. thaliana* and with the long tRNase Z enzymes from yeast and *Drosophila*. In addition we investigated the metal requirements for the reaction to determine whether bpNPP hydrolysis and pre-tRNA cleavage require the same properties of the tRNase Z enzyme.

The Eukaryotic tRNase Z AthTRZ1 Cleaves bpNPP. The bacterial tRNase Z from *E. coli* (EcoTrz) hydrolyzes bpNPP efficiently with a k_{cat} of 59 s^{-1} and a K_M of 4 mM (Table 1) (*16*). The reaction requires zinc ions and is not activated by iron or manganese ions (*16*). So far EcoTrz has been the only member of the tRNase Z proteins for which bpNPP kinetics have been studied in detail. Incubation of AthTRZ1 with bpNPP showed that the enzyme is also able to hydrolyze bpNPP but at a much lower efficiency than the tRNase Z from *E. coli* (Table 1). While the K_M value for AthTRZ1 was only twofold increased relative to that of the *E. coli* tRNase Z, the turnover rate was eightfold reduced

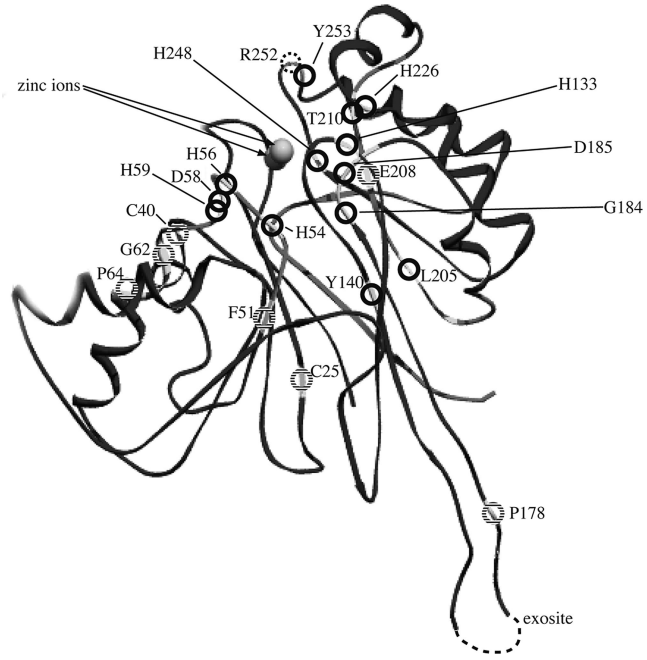

FIGURE 3: Location of mutations. The location of the mutations of the AthTRZ1 protein analyzed in this study are shown in the tRNase Z monomer. The AthTRZ1 amino acids have been superimposed onto the *B. subtilis* tRNase Z structure (*7*). Mutations which resulted in total loss of bpNPP activity are marked by a black circle. Mutations which showed reduced activity are marked by black and white striped circles. The R252 mutation, which has ten times the wild type activity, is shown with a dotted circle. The locations of the zinc ions, which are shown as gray spheres, are indicated by arrows. "Exosite" indicates the location of the exosite, which lies in the region that was not resolved in the *B. subtilis* tRNase Z structure and is marked by a dashed line. The term exosite describes an element outside the active site that participates in substrate binding (*21*).

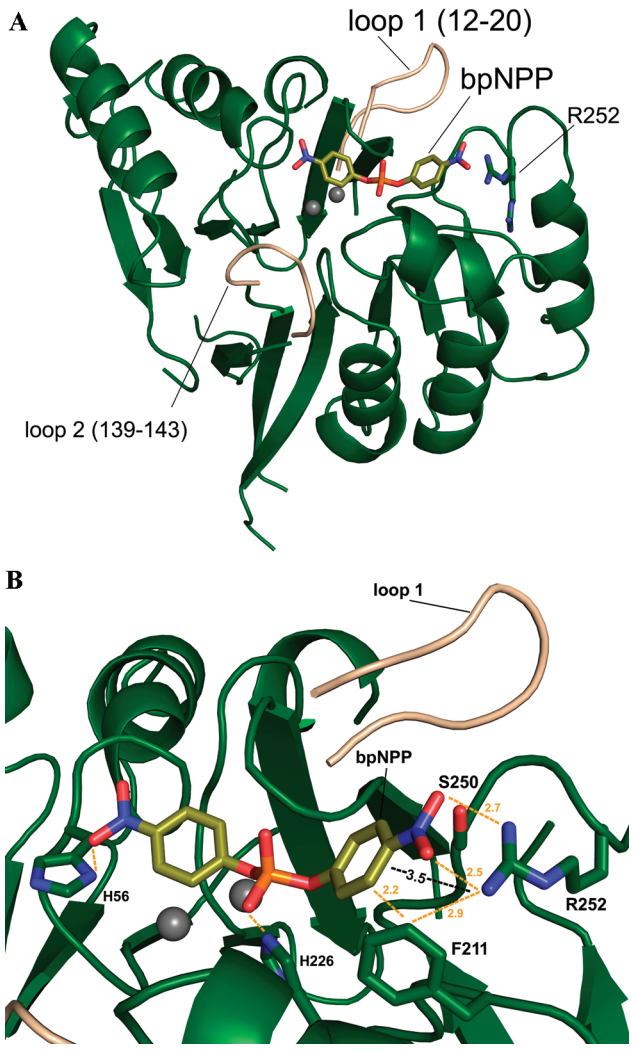

FIGURE 4: Model of bpNPP-binding to *A. thaliana* tRNase Z. A. Homology model of *A. thaliana* tRNase Z (green) in complex with bpNPP and targeted superposition with the *B. subtilis* tRNase Z (PDB ID 2FK6). Two equally probable conformations of arginine 252 showing its proximity to the bpNPP binding site are shown. The *B. subtilis* enzyme presents two protrusions (shown in beige: loop 1, *B. subtilis* residues 11−19; loop 2, *B. subtilis* residues 139−145) which are not present in AtTRZ1. Similar protrusions are found in the *E. coli* Trz (*9*). The bpNPP molecule was docked to the *A. thaliana* enzyme using the program PATCHDOCK and DOCK 6 and energy minimized. The molecules were superimposed using the program COOT, and the figure was generated using Pymol (*31*). B. Detailed illustration of the interactions between AthTRZ1 side chains and the ligand in its most energetically favorable position. Residues contacting bpNPP are shown in sticks. Distances shown in orange display close to medium length contacts. Distances shown in black give an approximate distance between the bpNPP phenyl group and the positively charged R252. All distances are given in Å.

(Table 1). However, these kinetic parameters still identify AthTRZ1 as an efficient catalyst of bpNPP hydrolysis.

Electrophoretic mobility shift assays (EMSA) with AthTRZ1 and tRNA in competition with bpNPP showed that addition of bpNPP does not interfere with tRNA binding (Figure 2A). Since pre-tRNAs were processed during the EMSA, resulting in ambiguous autoradiographs, EMSA experiments were carried out with the mature tRNA. The finding that bpNPP left tRNA binding unaffected is in agreement with previous reports indicating that tRNA recognition by Trz enzymes largely involves so-called exosites, modules, and domains distant from the active site (Figure 3) (*21*, *25*). To get an idea of the bpNPP binding site, we modeled the binding of bpNPP to AthTRZ1 (Figure 4). Notably, the enzyme-bpNPP recognition was modeled without any bias for the active site. As expected for a small substrate like bpNPP, its recognition does not involve exosite modules since it occupies only the active site. In previous studies deletion of Trz exosite modules abolished tRNA binding but only marginally interfered with bpNPP hydrolysis (*21*).

The tRNA processing reaction was inhibited by high concentrations of bpNPP (higher than 5 mM bpNPP at 15 nM pre-tRNA) whereas below these concentrations, pre-tRNA cleavage was not affected (Figure 2B). Addition of tRNA to the bpNPP reaction inhibited bpNPP cleavage, already at equimolar amounts (data not shown). These data suggest that inhibition of pre-tRNA processing by bpNPP and vice-versa occurs through active site competition. Furthermore these findings characterize bpNPP as an active-site directed probe, suitable to study Trz phosphodiesterase catalysis without exosite contributions.

Identification of Residues Important for bpNPP Hydrolysis. To identify amino acids important for catalysis of bpNPP hydrolysis, we analyzed the bpNPP hydrolysis activity of 22 variants of AthTRZ1 that have been generated in an earlier study (*17*). The AthTRZ1 variants carry single amino acid mutations in conserved positions (*17*). In addition to activity-screening, we determined the Michaelis−Menten type kinetic

Table 2: tRNase Z Variants[a]

mutation	bpNPP	pre-tRNA
AthTRZ1-wt	100 ± 6.8	100 ± 4.0
AthTRZ1-C25G	**52.7 ± 10.3**	**33.1 ± 7.7**
AthTRZ1-C40G	**41.9 ± 8.4**	**99.3 ± 13.2**
AthTRZ1-F51L	**31.1 ± 6.2**	**95.4 ± 12.3**
AthTRZ1-H54L	-	-
AthTRZ1-H56L	-	-
AthTRZ1-D58A	-	-
AthTRZ1-H59L	-	-
AthTRZ1-G62V	**10.8 ± 2.2**	**25.8 ± 3.9**
AthTRZ1-P64A	**62.2 ± 6.5**	**98.2 ± 7.9**
AthTRZ1-H133L	-	-
AthTRZ1-Y140L	-	**29.9 ± 2.2**
AthTRZ1-P178A	**24.3 ± 5.6**	**73.6 ± 8.1**
AthTRZ1-G184V	-	-
AthTRZ1-D185G	-	**6.7 ± 0.2**
AthTRZ1-L205I	-	**55.6 ± 1.1**
AthTRZ1-E208A	**54.1 ± 5**	**54.6 ± 1.0**
AthTRZ1-T210I	-	**85.1 ± 4.0**
AthTRZ1-H226L	-	-
AthTRZ1-H248L	-	-
AthTRZ1-R252G	**925.7 ± 5**	**26.0 ± 0.2**
deletion of R252	-	-
AthTRZ1-Y253S	-	**22.6 ± 3.3**

[a] Overview over the activity of the variants toward the substrate bpNPP. Column "mutation" indicates where the mutation was made, column "bpNPP": Percent activity of the bpNPP reaction, Calculated from the kcat values presented in Table 1, with wild type activity set to 100%, All AthTRZ1 variants were compared to the wild type activity. The pre-tRNA cleavage activity has been determined earlier (*17*) and is shown here in comparison to the bpNPP cleavage activities. Column pre-tRNA: Results from *in vitro* pre-tRNA processing experiments, wild type activity was set to 100%, All AthTRZ1 variants are quantified relative to the wild type activity (data taken from (*17*)). Variants which differ in their activity toward the two substrates are presented in boldface type.

parameters for those AthTRZ1 variants that possessed activity (Table 1).

From the 22 variants analyzed, 14 were not able to cleave bpNPP anymore (Table 2). Of these 14 variants, H59L and H248L were not able to form dimers (*17*); thus, their loss in catalytic activity is most likely due to an inability to fold properly. Five of the remaining twelve variants without bpNPP hydrolysis activity (Y140L, D185G, L205I, T210I, Y253S) were still able to process pre-tRNAs to some extent (*17*) (Table 2). Therefore, these individual amino acid exchanges (Y140L, D185G, L205I, T210I, Y253S) identify catalytically nonessential residues. Alternatively it might be that bpNPP and the scissile phosphodiester in the pre-tRNA do not align identically in the active site, such that they depend on nonidentical sets of contacts (Figure 5).

The structural analysis, based on the structure of the homologous enzyme BsuTrz, shows that Y253, like R252 (see below), is located at the entrance to the active site, T210 is located in proximity to the active site, and D185 acts as a bridging zinc ligand (Figure 3 and see below). L205 is located remotely from the active site and extends into the core of the enzyme structure. Its mutation to an isoleucine strongly interferes with bpNPP hydrolysis but has little effect on pre-tRNA processing. This situation is best explained by a structural distortion of the active site as a result of the isoleucine mutation, presumably through indirect destabilizing effects within the enzyme core. tRNA binding, on the other hand, through multiple interactions with the Trz enzymes, might lead to an "induced-fit" situation which

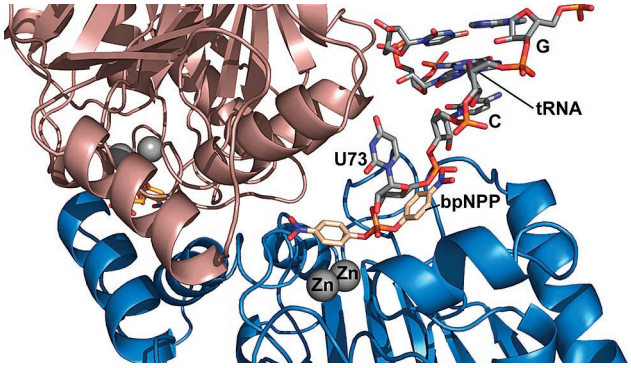

FIGURE 5: Comparison of pre-tRNA and bpNPP binding to tRNase Z. The crystal structure of the *B. subtilis* tRNase Z bound to tRNA was previously determined (*25*). The substrate bpNPP was docked onto this structure to compare binding of the two different substrates. Monomer A of the homodimeric tRNase Z enzyme is shown in blue and monomer B in brown. The two zinc ions are shown as gray spheres. The last three nucleotides of the tRNA are indicated (G71, C72, and U73). The bpNPP molecule was docked to the *B. subtilis* enzyme using the program PATCHDOCK and DOCK 6 and energy minimized. The figure was generated using the program Pymol (*31*).

restores the catalytically active form of the destabilized enzyme, allowing pre-tRNA processing.

Y140 does not directly contact bpNPP or the pre-tRNA. However, the residue is important for stability of the entire β sandwich region. Y140 occupies a central position with its hydrophobic ring π-stacking against Y91, F60, and F36. Mutating this tyrosine to leucine likely deprives the hydrophobic region of an essential bulky element for maintaining its stability. An additional effect may be variations in the protein's thumb which could in turn destabilize tRNA binding.

Mutations of the metal ligands H54, H56, D58, H59, H133, D185, and H248 resulted in no activity for bpNPP hydrolysis and, with the exception of D185, also for pre-tRNA processing (*17*), confirming the importance of these amino acids for active site chemistry.

Amino Acid Exchanges That Reduce the Catalytic Activity. Seven variants showed reduced activity (11−62% bpNPP hydrolysis activity) in comparison to the wild type protein (Table 2). Of these variants, three amino acid exchanges have a strong effect as indicated by a significantly altered K_M value (Table 1). P64A has a higher K_M whereas P178A and E208A show lower K_M values. With one exception (R252G), all amino acid exchanges resulted in a decreased catalytic constant k_{cat}. From a structural point of view, these findings are partially surprising, as P64 and P178 are located remotely to the active site (Figure 3).

A Single Amino Acid Exchange Results in Ten Times Higher Activity Compared to the Wild Type. The change of arginine 252 to a glycine residue had the most pronounced effect in this mutational study since the K_M value was fivefold lower and the turnover rate k_{cat} ninefold higher than for the wild type counterpart, resulting in a 44 times higher specificity constant (Table 1). Catalytic performance even exceeded that of the *E. coli* EcoTrz. R252 is in proximity to the metal binding pocket of the active site. A positively charged amino acid in this position might interact efficiently with the negatively charged tRNA but might repulse the hydrophobic phenol groups of the bpNPP molecule (Figure 4), thus explaining the divergent effects of this mutation on

Table 3: Metal Content of AthTRZ1[a]

protein	Mn	Zn
a.i. TRZ1	0.20 ± 0.01	1.30 ± 0.06
apo-TRZ1	0.13 ± 0.03	0.76 ± 0.13
TRZ1-Mn	2.47 ± 0.31	0.92 ± 0.16
TRZ1-Zn	0.21 ± 0.02	1.43 ± 0.26

[a] The metal content of AthTRZ1 as isolated (a.i. TRZ1) chelator-treated AthTRZ1 (apo-TRZ1) and metal-loaded AthTRZ1 proteins (TRZ1-Mn, loaded with manganese, TRZ1-Zn, loaded with zinc) were determined with ICP-MS and ICP-OES. Column Mn shows the manganese content of the respective protein and column Zn the zinc content. The metal content is given in atoms per dimer.

bpNPP hydrolysis and pre-tRNA processing. Chemosterically a glycine in position 252 is acceptable and would likely create a double effect: increased flexibility allowing easier substrate access, but also an increased degree of instability, particularly in the absence of substrate, since R252 also contacts Ser250 (2.6 Å, distance not shown in the figure), which is part of the bpNPP stabilization. The void created by the absence of R252 may also not shield the hydrophobic pocket well enough, creating an increased need to fill the gap.

The importance of residue R252 has been shown earlier; according to the cocrystallization of *B. subtilis* tRNase Z together with tRNA, R252 (the *B. subtilis* equivalent is R273) acts as a bridge between the tRNA and the protein (*25*). This arginine was also discussed as a candidate for signaling the presence of the tRNA in the dimer and initiating the conformational changes to stabilize this region (*25*).

Long tRNase Z Enzymes Do Not Cleave bpNPP. To date only short tRNase Z enzymes have been analyzed with respect to their activity toward bpNPP. To investigate whether long tRNase Z enzymes are also competent to cleave bpNPP, we incubated the yeast long tRNase Z (Trz1p) and the *Drosophila* long tRNase Z (DmeTrz) with bpNPP. Although both long tRNase Z enzymes have been shown to be competent in pre-tRNA processing (*20*, *21*, *26*), we did not observe any hydrolysis of the small substrate bpNPP (data not shown). However, pre-tRNA processing by the two enzymes was inhibited by bpNPP concentrations higher than 10 mM (Figure 2C). This is a surprising observation, suggesting that on the one hand this small substrate occupies the catalytic center in the long tRNase Z proteins thereby preventing pre-tRNA cleavage but on the other hand it is obviously not positioned correctly to be processed.

Major differences in reactivity toward the bpNPP substrate exist also between the short tRNase Z enzymes AthTRZ1 and EcoTrz (Table 1). However, mutation of a single amino acid (R252) converted AthTRZ1 into an enzyme even more active than EcoTrz. Thus, even slight changes in the protein structure can drastically alter the reactivity toward the small phosphodiester bpNPP.

AthTRZ1 Binds Zn^{2+} Ions Very Tightly. To analyze whether AthTRZ1 requires metal ions for the different activities, we intended to fully deplete the enzyme from intrinsic metal ions. For these purposes, the AthTRZ1 protein was incubated with EDTA and the very high affinity chelator TPEN (for Zn^{2+} $K\alpha = 10^{16}$ M^{-1}) (*27*). When the enzyme was analyzed for residual metal content after dialysis, 0.76 Zn^{2+} ions per dimer (0.38 per monomer) were detected in AthTRZ1 (Table 3). A similar tight affinity for Zn^{2+} ions

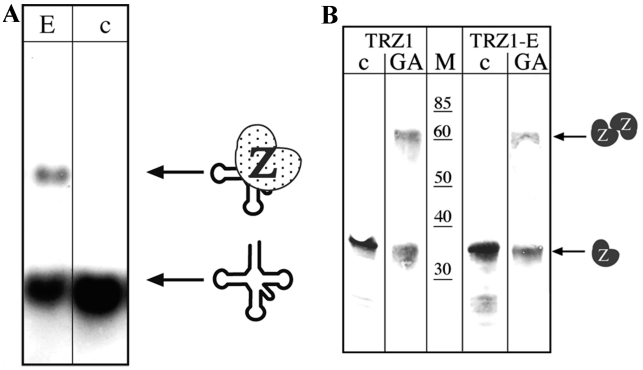

FIGURE 6: A. Metal ions are not required for tRNA binding. The chelator-treated AthTRZ1 was incubated with wheat tRNA to analyze whether the protein binds to tRNA without addition of metal ions. The reaction was loaded onto a nondenaturing polyacrylamide gel, which was subsequently analyzed by autoradiography. The autoradiograph clearly shows that chelator-treated AthTRZ1 still binds to tRNA. Lane E: chelator-treated TRZ1 incubated with tRNA; lane c: control without addition of proteins. The tRNA and the tRNA/protein complex are shown at the right schematically. B. Metal ions are not required for dimer formation. AthTRZ1 and chelator-treated AthTRZ1 were incubated with glutaraldehyde, separated on an SDS PAGE, and transferred to a western membrane. Monomers and dimers were detected with anti-TRZ1 antibodies. Both proteins form dimers. Lanes c show the control to which glutaraldehyde was not added; lanes GA show the reaction with glutaraldehyde. Lane TRZ1: TRZ1; lane TRZ1-E: chelator-treated TRZ1. A protein size marker is shown in kDa. TRZ1 monomer and dimer are shown schematically at the right.

has been observed for the other RNA processing metallo-β-lactamase enzyme CPSF-73 (*28*). In contrast, EDTA treatment of *E. coli* TRZ1 yielded 0.14 Zn^{2+} per dimer (*16*). The residual Zn^{2+} content of chelator-treated AthTRZ1 was sufficient for bpNPP hydrolysis (Supporting Information Figure 1) but insufficient for tRNA processing (*17*), in line with the observation that even EDTA treatment alone results in loss of the tRNA processing activity (*17*, *29*). Electrophoretic mobility shift assays demonstrated that chelator-treated tRNase Z is still able to bind tRNA (Figure 6A); thus, the retained zinc ion is sufficient to allow binding at least of the processed product (the tRNA). Additionally, cross-linking experiments with glutaraldehyde showed that the chelator-treated enzyme still forms dimers although to a lesser extent than the untreated AthTRZ1 (Figure 6B).

To reveal how many metal ions can be bound to AthTRZ1, we loaded the chelator-treated enzyme either with Mn^{2+} or Zn^{2+}. Proteins loaded in such a way were analyzed using inductively coupled plasma mass spectrometry (ICP-MS) and inductively coupled plasma optical emission spectroscopy (ICP-OES) (Table 3). The metal content determined for the Mn^{2+}-loaded AthTRZ1 was 2.47 Mn^{2+} ions per dimer and 0.92 Zn^{2+} ions per dimer. In the Zn^{2+}-loaded enzyme, 1.43 Zn^{2+} ions and 0.21 Mn^{2+} ions were found per dimer (see below).

Metal Ion Requirements for Pre-tRNA and bpNPP Cleavage. To analyze which metal ions are required for the hydrolysis of bpNPP, reactions were carried out in metal-free buffer with the chelator-treated enzyme (with 0.76 Zn^{2+} ions per dimer). The chelator-treated enzyme remained capable of hydrolyzing bpNPP to the same extent as the "as isolated" enzyme, which contains 2.6 Zn^{2+} ions per dimer (Supporting Information Figure 1). Thus, the 0.76 zinc^{2+} ions per dimer retained by the enzyme after chelator treatment

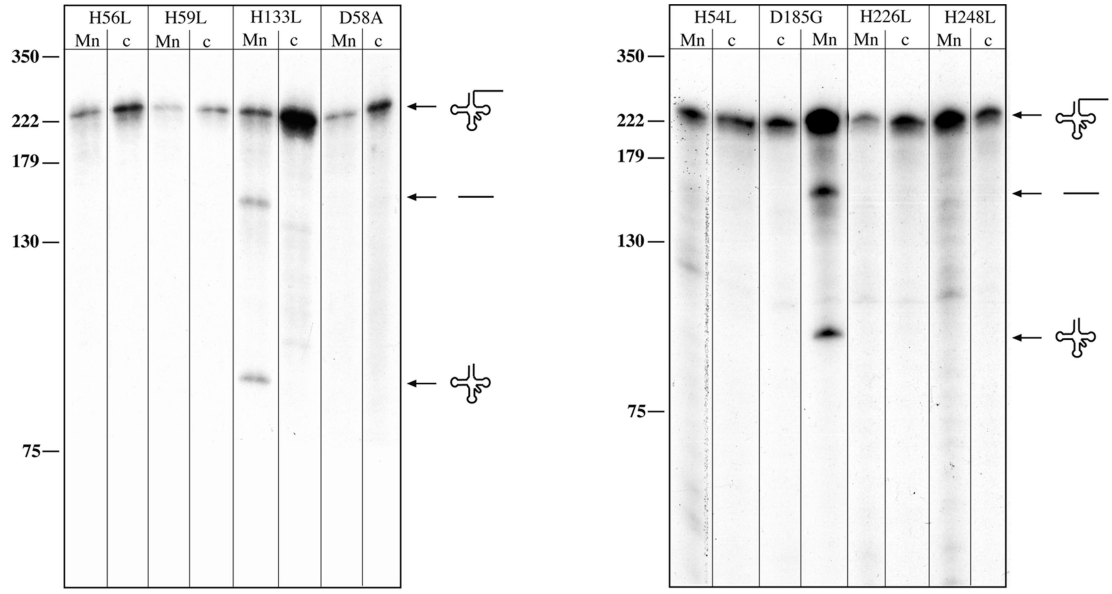

FIGURE 7: Rescue of catalytic activity of AthTRZ1 variants. AthTRZ1 variants were metal-depleted with EDTA and TPEN, and the chelator-treated enzyme was subsequently incubated with manganese in *in vitro* processing reactions. Variants H54L, H56L, D58A, H59L, H133L, D185G, H226L, and H248L remained catalytically inactive upon incubation with magnesium (*17*, *32*). However, addition of manganese rescues the activity of variant H133 and D185. Lane m: DNA size marker (sizes are indicated in nucleotides at the left); lane c: control reaction without addition of proteins. Precursor and products are shown schematically at the right.

are sufficient for bpNPP hydrolysis. We then added Mg^{2+}, Ca^{2+}, Mn^{2+}, Fe^{2+}, or Zn^{2+} to the bpNPP reaction. Whereas Mg^{2+}, Ca^{2+}, and Fe^{2+} did not influence the bpNPP hydrolysis, Mn^{2+} and Zn^{2+} increased bpNPP cleavage 3-fold and 2-fold, respectively (Supporting Information Figure 1).

Comparison of the metal requirements for bpNPP hydrolysis and pre-tRNA processing indicates the requirement of additional metal ions for tRNA processing. While pre-tRNA cleavage is catalyzed when manganese, magnesium, or calcium is added to the chelator-treated enzyme (*17*, *18*), bpNPP hydrolysis is enhanced upon addition of either manganese or zinc ions. However, zinc alone is not sufficient to rescue pre-tRNA processing (*17*), indicating differences in the metal ion requirements for the bpNPP hydrolysis and the pre-tRNA processing reaction. Since magnesium and calcium can rescue tRNA processing, a structural role of these metal ions is likely. As chelator-treated tRNase Z still binds tRNA molecules in EMSA (Figure 6A), this structural role might be involved in the correct positioning of the pre-tRNA for catalysis. However, we cannot fully exclude that the different metal requirements reflect more fundamental differences in the mechanism of phosphodiester hydrolysis reactions.

Pre-tRNA Processing of Catalytically Inactive TRZ1 Variants Can Be Rescued by Addition of Manganese. To investigate whether tRNase Z variants, which are catalytically inactive toward bpNPP hydrolysis, can be rescued by addition of metal ions, we depleted the mutant proteins H54L, H56L, D58A, H59L, H133L, D185G, H226L, and H248L of metal ions as described above and incubated them with Mg^{2+} and Mn^{2+} ions. Neither Mg^{2+} nor Mn^{2+} ions were able to rescue the bpNPP hydrolysis activity of the variants. Since these variants were also inactive in pre-tRNA processing (*17*), we tested whether addition of Mg^{2+} and Mn^{2+} ions rescues pre-tRNA processing. Manganese ions rescued the *in vitro* tRNA processing activity of two variants: H133L and D185G (Figure 7).

For the *B. subtilis* tRNase Z, it was suggested that interaction of the tRNA with the protein induces a change of conformation that moves the amino acids H226, H133, and D185 (in *B. subtilis*: H247, H140, and D211 (*25*)) into the active site. Thus, H133 and D185 of AthTRZ1 might be located in the active site taking part in catalysis or in substrate positioning. The fact that only tRNA processing and not bpNPP cleavage activity of the H133L and D185G variants can be rescued upon addition of Mn^{2+} suggests that pre-tRNA binding induces correct folding of AthTRZ1. In this respect, Mn^{2+} may mediate the protein−tRNA interaction as well as having a structural role in either AthTRZ1 or the tRNA molecule.

For the *Thermotoga maritima* tRNase Z (TmaTrz), similar assays were performed, and defects caused by mutation of H134 and D190 (corresponding to H133 and D185 in AtTRZ1) could also be rescued by addition of Mn^{2+} (*30*). But altogether the results of the *Thermotoga* study are difficult to compare since the authors did not treat the enzymes with chelators before analyzing the metal dependency and did not determine the metal content of the *Thermotoga* enzyme at any point (*30*).

Metal Requirements for tRNase Z Enzymes in Comparison to Other Metallo-β-lactamases. The present study identifies AthTRZ1 as a tight zinc binder, in contrast to EcoTrz which is easily deprived of metal ions (*16*). Besides the tightly bound Zn^{2+} ion, AthTRZ1 requires additional metal ions for pre-tRNA processing (Mn^{2+}, Ca^{2+}, or Mg^{2+}). In contrast, bpNPP hydrolysis by chelator-treated AthTRZ1 occurs without addition of metal ions but is stimulated two- to threefold when free Mn^{2+} or Zn^{2+} ions are added (Supporting Information Figure 1). For bpNPP hydrolysis, we suspect that active site bound metal ions participate in phosphodiester hydrolysis but not in substrate recognition. Pre-tRNA processing but not tRNA binding requires additional Mn^{2+} or Mg^{2+} (see EMSA, Figure 6A) which might be necessary for correct substrate positioning. In this regard, Mn^{2+} may

play a dual role by taking part both in substrate positioning and phosphodiester hydrolysis. Mn^{2+} is a known substitute for Mg^{2+} in nucleic acid interactions while it also catalyzes hydrolytic reactions in metalloenzymes like glyoxalase II. We suspect that the different roles of Mn^{2+} take place at different locations on the enzyme. In fact, the Mn^{2+}-loaded enzyme contains more than 2 Mn^{2+} in contrast to less than 2 Zn^{2+} for the Zn^{2+}-loaded enzyme. While Zn^{2+} binding may be restricted to the active site, Mn^{2+} could be located in the active site and at additional locations. Noteworthy, the present dual substrate approach is ideally suited to yield this functional dissection of the involvement of different metal ions.

The present study identifies AthTRZ1 as an efficient catalyst of bpNPP hydrolysis and applies this new finding to the functional characterization of a mutational library of AthTRZ1. Together with a recent study (*17*), this yields a comprehensive, dual-substrate mutational map of AthTRZ1 with unexpected insights into both bpNPP hydrolysis and pre-tRNA processing.

ACKNOWLEDGMENT

We would like to thank Elli Bruckbauer and Ingrid Schleyer for expert technical assistance and Patrick Beaudette for proofreading the manuscript.

SUPPORTING INFORMATION AVAILABLE

Supporting Information Figure 1 showing the metal requirements of the bpNPP reaction. The bpNPP activity of the chelator-treated AthTRZ1 without (TRZ-E) and with additional metal ions (Zn^{2+}, Fe^{2+}, Mn^{2+}, Ca^{2+}, Mg^{2+}, K^{2+}) has been tested. The chelator-treated AthTRZ1 without additional metal ions has the same activity as the non-chelator-treated AthTRZ1 (data not shown). Addition of Zn^{2+} ions to the chelator-treated enzyme almost doubles the activity and addition of Mn^{2+} ions triples the activity. This material is available free of charge via the Internet at http://pubs.acs.org.

REFERENCES

1. Vogel, A., Schilling, O., Späth, B., and Marchfelder, A. (2005) The tRNase Z family of proteins. Physiological functions, substrate specificity and structural properties, *Biol. Chem. 386*, 1253−1264.
2. Schiffer, S., Rösch, S., and Marchfelder, A. (2002) Assigning a function to a conserved group of proteins: the tRNA 3′-processing enzymes, *EMBO J. 21*, 2769−2777.
3. Tavtigian, S. V., Simard, J., Teng, D. H., Abtin, V., Baumgard, M., Beck, A., Camp, N. J., Carillo, A. R., Chen, Y., Dayananth, P., Desrochers, M., Dumont, M., Farnham, J. M., Frank, D., Frye, C., Ghaffari, S., Gupte, J. S., Hu, R., Iliev, D., Janecki, T., Kort, E. N., Laity, K. E., Leavitt, A., Leblanc, G., McArthur-Morrison, J., Pederson, A., Penn, B., Peterson, K. T., Reid, J. E., Richards, S., Schroeder, M., Smith, R., Snyder, S. C., Swedlund, B., Swensen, J., Thomas, A., Tranchant, M., Woodland, A. M., Labrie, F., Skolnick, M. H., Neuhausen, S., Rommens, J., and Cannon-Albright, L. A. (2001) A candidate prostate cancer susceptibility gene at chromosome 17p, *Nat. Genet. 27*, 172−180.
4. Vogel, A., Schilling, O., and Meyer-Klaucke, W. (2004) Identification of metal binding residues for the binuclear zinc phosphodiesterase reveals identical coordination as glyoxalase II, *Biochemistry 43*, 10379−86.
5. Aravind, L. (1999) An evolutionary classification of the metallo-beta-lactamase fold proteins, *In Silico Biol. 1*, 69−91.
6. Daiyasu, H., Osaka, K., Ishino, Y., and Toh, H. (2001) Expansion of the zinc metallo-hydrolase family of the beta-lactamase fold, *FEBS Lett. 503*, 1−6.
7. de la Sierra-Gallay, I. L., Pellegrini, O., and Condon, C. (2005) Structural basis for substrate binding, cleavage and allostery in the tRNA maturase RNase Z, *Nature 433*, 657−661.
8. Ishii, R., Minagawa, A., Takaku, H., Takagi, M., Nashimoto, M., and Yokoyama, S. (2005) Crystal structure of the tRNA 3′ processing endoribonuclease tRNase Z from Thermotoga maritima, *J. Biol. Chem. 280*, 14138−14144.
9. Kostelecky, B., Pohl, E., Vogel, A., Schilling, O., and Meyer-Klaucke, W. (2006) The crystal structure of the zinc phosphodiesterase from Escherichia coli provides insight into function and cooperativity of tRNase Z-family proteins, *J. Bacteriol. 188*, 1607−1614.
10. Minvielle-Sebastia, L., and Keller, W. (1999) mRNA polyadenylation and its coupling to other RNA processing reactions and to transcription, *Curr. Opin. Cell Biol. 11*, 352−7.
11. Wolter, R., Siede, W., and Brendel, M. (1996) Regulation of SNM1, an inducible Saccharomyces cerevisiae gene required for repair of DNA cross-links, *Mol. Gen. Genet. 250*, 162−8.
12. Pannicke, U., Ma, Y., Hopfner, K. P., Niewolik, D., Lieber, M. R., and Schwarz, K. (2004) Functional and biochemical dissection of the structure-specific nuclease ARTEMIS, *EMBO J. 23*, 1987−97.
13. Francis, S. H., Turko, I. V., and Corbin, J. D. (2001) Cyclic nucleotide phosphodiesterases: relating structure and function, *Prog. Nucleic Acid Res. Mol. Biol. 65*, 1−52.
14. Schilling, O., Vogel, A., Kostelecky, B., Natal da Luz, H., Spemann, D., Späth, B., Marchfelder, A., Tröger, W., and Meyer-Klaucke, W. (2005) Zinc- and iron-dependent cytosolic metallo-beta-lactamase domain proteins exhibit similar zinc-binding affinities, independent of an atypical glutamate at the metal-binding site, *Biochem. J. 385*, 145−153.
15. Schilling, O., Wenzel, N., Naylor, M., Vogel, A., Crowder, M., Makaroff, C., and Meyer-Klaucke, W. (2003) Flexible metal binding of the metallo-beta-lactamase domain: glyoxalase II incorporates iron, manganese, and zinc in vivo, *Biochemistry 42*, 11777−11786.
16. Vogel, A., Schilling, O., Niecke, M., Bettmer, J., and Meyer-Klaucke, W. (2002) ElaC encodes a novel binuclear zinc phosphodiesterase, *J. Biol. Chem. 277*, 29078−85.
17. Späth, B., Kirchner, S., Vogel, A., Schubert, S., Meinlschmidt, P., Aymanns, S., Nezzar, J., and Marchfelder, A. (2005) Analysis of the functional modules of the tRNA 3′ endonuclease (tRNase Z), *J. Biol. Chem. 280*, 35440−35447.
18. Späth, B. (2005), Ulm University, Ulm, Germany.
19. Gill, S. C., and von Hippel, P. H. (1989) Calculation of protein extinction coefficients from amino acid sequence data, *Anal. Biochem. 182*, 319−26.
20. Dubrovsky, E. B., Dubrovskaya, V. A., Levinger, L., Schiffer, S., and Marchfelder, A. (2004) Drosophila RNase Z processes mitochondrial and nuclear pre-tRNA 3′ ends in vivo, *Nucleic Acids Res. 32*, 255−62.
21. Schilling, O., Späth, B., Kostelecky, B., Marchfelder, A., Meyer-Klaucke, W., and Vogel, A. (2005) Exosite modules guide substrate recognition in the ZiPD/ElaC protein family, *J. Biol. Chem. 280*, 17857−17862.
22. Schneidman-Duhovny, D., Inbar, Y., Polak, V., Shatsky, M., Halperin, I., Benyamini, H., Barzilai, A., Dror, O., Haspel, N., Nussinov, R., and Wolfson, H. J. (2003) Taking geometry to its edge: fast unbound rigid (and hinge-bent) docking, *Proteins 52*, 107−12.
23. Kuntz Laboratory, University of California, San Francisco.
24. Emsley, P., and Cowtan, K. (2004) Coot: model-building tools for molecular graphics, *Acta Crystallogr. Sect. D: Biol. Crystallogr. 60*, 2126−32.
25. Li de la Sierra-Gallay, I., Mathy, N., Pellegrini, O., and Condon, C. (2006) Structure of the ubiquitous 3′ processing enzyme RNase Z bound to transfer RNA, *Nat. Struct. Mol. Biol. 13*, 376−377.
26. Takaku, H., Minagawa, A., Takagi, M., and Nashimoto, M. (2003) A candidate prostate cancer susceptibility gene encodes tRNA 3′ processing endoribonuclease, *Nucleic Acids Res. 31*, 2272−2278.
27. Jakob, U., Eser, M., and Bardwell, J. C. (2000) Redox switch of hsp33 has a novel zinc-binding motif, *J. Biol. Chem. 275*, 38302−10.
28. Mandel, C. R., Kaneko, S., Zhang, H., Gebauer, D., Vethantham, V., Manley, J. L., and Tong, L. (2006) Polyadenylation factor CPSF-73 is the pre-mRNA 3′-end-processing endonuclease, *Nature 444*, 953−6.
29. Mayer, M., Schiffer, S., and Marchfelder, A. (2000) tRNA 3′ processing in plants: nuclear and mitochondrial activities differ, *Biochemistry 39*, 2096−2105.

30. Minagawa, A., Takaku, H., Ishii, R., Takagi, M., Yokoyama, S., and Nashimoto, M. (2006) Identification by Mn2+ rescue of two residues essential for the proton transfer of tRNase Z catalysis, *Nucleic Acids Res. 34*, 3811−3818.
31. DeLano, W. L. DeLano Scientific LLC, San Carlos, CA.
32. Settele, F. (2006), University of Ulm, Ulm, Germany.

BI7010459